HHS Public Access

Author manuscript

*ACS Appl Bio Mater*. Author manuscript; available in PMC 2022 January 06.

Published in final edited form as:

*ACS Appl Bio Mater*. 2019 March 18; 2(3): 1262–1269. doi:10.1021/acsabm.8b00818.

# Self-assembled DNA-THPS hydrogel as a topical antibacterial agent for wound healing

**Xingxing Jiang**[†], **Man Li**[†], **Xiaoxi Guo**[‡], **Minghui Yang**[†], **Avraham Rasooly**[§]

[†]College of Chemistry and Chemical Engineering, Central South University, Changsha, Hunan 410083, P. R. China

[‡]College of Chemistry and Chemical Engineering, Qufu Normal University, Qufu, Shandong 273165, P. R. China

[§]National Cancer Institute, National Institutes of Health, Rockville, Maryland 20850, United States

## Abstract

We report a novel and potential wound dressing hydrogel based on DNA and a green industrial microbiocide tetrakis (hydroxymethyl) phosphonium sulfate (THPS) via one-pot self-assembly. Intermolecular electrostatic interaction and hydrogen bonding between DNA and THPS together drive the formation of the adhesive DNT (DNA+THPS) hydrogel, featuring with self-healing, shear-thinning and injectability. This wound dressing hydrogel possesses broad-spectrum antibacterial ability with low cytotoxicity to L929 cells. Furthermore, the wound dressing can reduce the risk of wound infection by releasing THPS to suppress bacterial spread and accelerate wound healing. The low cost and simple preparation may make the hydrogel attractive in biomedical applications and could be a good reference to others.

## Graphical Abstract

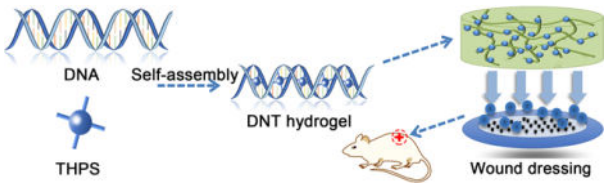


Self-assembled DNT hydrogel drove by intermolecular electrostatic interaction and hydrogen bonding is able to behave as an excellent wound dressing to against bacteria and accelerate wound healing. Its contact-killing mechanism makes it easy to kill bacteria in a broad-spectrum way. Facile preparation and outstanding efficacy would offer a solution to eliminate the problem of bacterial drug resistance.

Corresponding author: M. Yang. yangminghui@csu.edu.cn, A. Rasooly. rasoolya@mail.nih.gov.

The authors declare no competing financial interest.

## INTRODUCTION

Bacterial wound infection not only affects the wound healing but also poses threats of systemic infection sepsis as well as organ failure, which are potentially life-threatening.[1] Traditional wound treatments were always involve the utilization of antibiotics, such as over-the-counter Neosporin, a triple-antibiotic ointment with bacitracin, neomycin and polymyxin b. However, overuse antibiotics may contribute to the spread of antibiotic resistance,[2] and may arise biosafety concerns. Such antimicrobial resistance is a growing health threat, reducing the ability to prevent and treat of bacteria infectious diseases. To address this challenge, massive efforts have been dedicated to develop non-conventional antibacterial treatments, significant antibacterial materials were proposed as alternatives to antibiotics, including reintroduction of historical broad-spectrum agents such as silver,[3] copper,[4] gold[5] or natural products[6] and narrow-spectrum agents like bacteriophages[7] or peptides.[8] In addition, engineering the antibacterial agent in to hydrogel or assembling it into hydrogel matrices are capable of realizing the sustained release. The ‘functional hydrogels’ not only have developed antibacterial properties but also work as dressings to accelerate wound healing. To effectively avoid wound infection and promote the wound healing, antibacterial agents are often embedded onto the supports to form wound dressing for controllable and lasting release. One type of supports widely used for antimicrobial agents are hydrogels. Hydrogels are highly absorbent hydrophilic network of polymer chains and have been demonstrated as excellent supports for drug delivery due to their biodegradability and biocompatibility and are used for tissue engineering,[9] cell culture,[10] drug delivery[11] as well as contact lenses.[12] They are also widely used for wound healing as adhesive dressing systems to provide moisture to wounds and absorb exudate, function as obstruction to bacteria that provide a barrier against the external threats.[13] Recently, self-assembled biomacromolecule hydrogels including peptides, proteins, keratins, polysaccharide like chitosan,[14] self-assembled tea tannin,[15] bacterial cellulose (BC)/acrylic acid (AA) hydrogels[16] or antimicrobial honey-based hydrogel[17] were studied for a broad array of biomedical applications. Compared with these biomacromolecules mentioned above, DNA, as a natural polymer, can be a perfect polymeric candidate for hydrogel formation due to its high molecular weight and unique properties like shape control and cell free production,[18] Which advantages over other synthetic or natural polymer such as poly (ethylene glycol), alginate and hyaluronic acid.[19] Thus, it is desirable to develop DNA-based antibacterial hydrogel to meet the increasing biomedical requirement.

There has been great interest in preparing DNA hydrogels in the past decades and have presented as an interesting material and they have, for example, been explored as antigen delivery system,[20] switchable material for aptamer-based fluorescent detection[21] and delivery vehicle for light-triggered cancer therapy.[22] Moreover, DNA hydrogels can be rationally designed for advanced shaping approaches such as magnetic field[23] or 3D printing.[24] Noncovalent bond like complementary base-pairing, blending with cationic polymers and covalent bond were typically used to prepare DNA hydrogels.[25–27]In contrast to the complementary base-pairing exploited widely for DNA hydrogels formation, small organic molecules or metal ions can physically cross-link DNA via noncovalent bond, which involve electrostatic interaction, groove combination and intercalation.[28] such DNA

hydrogels were reported to snare carcinogens like polycyclic aromatic hydrocarbons (PAHs) through intercalation,[29] which inspired us to use these physical interactions to develop novel bioinspired materials.

Herein, we propose a new potential antimicrobial agent to combine with DNA to fabricate DNA-based hydrogel. Tetrakis (hydroxymethyl) phosphonium sulfate (THPS), a cationic phosphonium salt, has attracted extensive industrial and agricultural interest as a pesticide and broad-spectrum microbiocide for water treatment. It can inhibit the growth of microorganisms including bacteria, algae, and fungi[30–34] and produce no mutagenic response,[35] owing to its potent antibacterial efficacy, environmental safety and low toxicity. Because of that it was awarded the American Green Chemical Award from Environmental Protection Agency (EPA) in 1997.[36] In this study, THPS was proved to be capable of cross-linking DNA by taking advantage of intermolecular electrostatic interaction and hydrogen bonding. DNA played roles of hydrogelator and building block while THPS was used as a trigger and antibacterial ability donor in the formation of the obtained hydrogel, which named as DNT hydrogel. In this way, THPS could achieve the lasting and controllable release at the same time. More importantly, the obtained DNT hydrogels are endowed with excellent antibacterial ability, which could be implemented as antibacterial coatings for the wound infections caused by bacteria and may provide a solution to antibiotic resistance.

## RESULT AND DISCUSSION

### Self-assembly and characterizations of DNT hydrogels.

The formation procedure of DNT hydrogel is shown in Figure 1a. First, 4 wt% DNA was dissolved in deionized water (950 μL) and heated at 90 °C for about 20 minutes, then 50 mg $mL^{-1}$ (50 μL) THPS was introduced and the transparent DNT hydrogel was obtained finally (Figure 1b). No gelation was observed when DNA concentration is lower than 2 wt%. (Table S1). Frequency-dependent oscillatory rheology of the DNT hydrogels showed that G' surpassed G" throughout the whole frequency sweep tested at a constant strain of 1%, confirming the formation of hydrogel (Figure 1c). In addition, the intertwined network and porous structure of the lyophilized hydrogel were visualized by Scanning electron microscopy (SEM) (Figure 1d).

THPS is a positively charged sulfate salt and rich in -OH functional groups (Figure S1), which can interact with the phosphate backbone of DNA via intermolecular electrostatic interaction. Besides, THPS, as a small organic molecule, can take advantage of its molecular rotation to combine with nitrogenous bases in the groove of DNA via hydrogen bonding. Based on these speculations, we assumed that the hydrogelation was achieved by intermolecular electrostatic interaction and hydrogen bonding. To verify our assumptions, we first employed Circular Dichroism (CD) spectrum to investigate the structural information of the DNA and DNA-THPS complex in water. As shown in Figure 2a, a pair of CD signals at 245 and 275 nm were observed (inset in Figure 2a), indicating the right-handed double helix structure of DNA in B conformation.[37] When THPS was introduced, the peak at 275 nm was shifted to longer wavelength. Noticeably, the intensity was decreased gradually with the increasing of THPS concentration from 0 to 50 mg $mL^{-1}$, illustrating the introduction of THPS leads to the gradual transition of DNA strand from

B-form to C-form.[38, 39] A large proportion of the DNA phosphates were neutralized by site binding the cations because of electrostatic effects, resulting in this transition.[40] For UV-vis absorption spectra, the absorption peak centered at 260 nm was DNA absorption band (Figure 2b). After mixing with THPS, an evident hypochromicity of DNA absorption band was observed. Hence, the introduction of THPS can be implemented as a block to prevent nitrogenous bases from being exposed in a groove combination manner, leading to the hypochromicity.[41]

We then used Fourier transform infrared (FTIR) spectroscopy to study the role of intermolecular hydrogen bonding in the formation of the hydrogel. As shown in Figure 2c, vibrational bands at 1700, 1640, 1531 and 1487 $cm^{-1}$ are assigned to guanine (G) , thymine (T) , adenine (A) and cytosine (C) nitrogenous bases of DNA solution, respectively.[42] Upon hydrogelating with THPS, guanine band peak shifted from 1700 to 1685 $cm^{-1}$ and thymine band peak shifted from 1640 to 1629 $cm^{-1}$. Additionally, peak positions of adenine (A) and cytosine (C) stayed almost unchanged and too weak to be shown, mostly because of the strong peak intensity of THPS at this wavenumber range. This result demonstrated that THPS was most likely to combine with guanine (G) and thymine (T) nitrogenous bases via hydrogen bonding in a groove combination manner in this system.[43] The wavenumber where the asymmetric vibrations of phosphate group initially appeared was 1238 $cm^{-1}$ when the DNA was alone,[19, 44] after hydrogelated with THPS , this peak was significantly shifted to 1182 $cm^{-1}$. Meanwhile, the symmetric vibrations of phosphate group detected at 1094 $cm^{-1}$ was shifted to 1044 $cm^{-1}$, suggesting the strong intermolecular electrostatic interaction between THPS and DNA.[45] Therefore, FITR analysis verified the intermolecular electrostatic interaction and hydrogen bonding within the DNT hydrogel.

Finally, to further confirm these results, molecular docking was carried out by AutoDockTools (4.2.26) to mimic the binding sites of THPS to DNA in this system, the conformation with the lowest binding energy at −3.0 eV was chosen for molecular docking simulations after 100 times test (Figure S2). As shown in Figure 2d, THPS combined with thymine (T) and guanine (G) nitrogenous bases in a groove bonding manner via hydrogen bonding. According to these spectroscopic results and molecular docking simulations, it can be concluded that the intermolecular electrostatic interaction and hydrogen bonding drove the formation of DNT hydrogel together.

## Antibacterial performance and in vitro biocompatibility of DNT hydrogels.

We explored the antibacterial activity of the DNT hydrogels by contacting with bacteria with Optical Density (OD) measurement. In particular, Gram-positive bacteria *Staphylococcus aureus* (*S. aureus*) and Gram-negative bacteria *Escherichia coli* (*E. coli*) as model bacteria for assessment in our experiment. Time-dependent antibacterial tests of hydrogels against *S. aureus* and *E. coli* were shown in Figure 3a and Figure 3b, respectively. It was observed that DNT hydrogels and THPS completely restrained the bacterial growth of *S. aureus* and *E. coli*. In sharp contrast, bacteria displayed significant growth in samples with DNA solution or without DNT hydrogels (control). In addition, both *S. aureus* and *E. Coli* samples cultured with liquid culture medium and DNA solution flourished on the Luria-Bertani (LB) solid plates, but counterparts contacted with hydrogel were all dead and did not proliferate

on the LB solid plates (Figure S3). We also used Mass Spectrum (MS) to verify the release of THPS from DNT hydrogel (Figure S4). These results demonstrated the release of THPS from DNT hydrogel is responsible for this phenomenon. Besides, we systematically evaluated antibacterial capacities of the DNT hydrogel towards various concentrations of *S. aureus* and *E. coli*. As shown in Figure 3c and Figure 3d, the hydrogels were able to inhibit up to $1\times10^9$ colony-forming units (CFU) per milliliter of *S. aureus* and *E. coli* proliferation, demonstrating its excellent broad-spectrum bactericidal ability. All results showed the DNT hydrogels own outstanding broad-spectrum antimicrobial ability.

We also investigated the in vitro biocompatibility of DNT hydrogels. L929 cells were contacted with the hydrogel for 2 d with the tissue culture polystyrene dish as control. The CCK-8 absorbance is inversely proportion to the cytotoxicity and we found that the CCK-8 absorbance at 450 nm was almost same with the control (Figure 3e), illustrating DNT hydrogel exhibited an excellent biocompatibility. Additionally, L929 cells contacted with the hydrogel were found to show normal and healthy morphologies (Figure 3f). These observations suggested that the hydrogel was in vitro biocompatible toward normal mammalian cells.

## Antibacterial mechanism of DNT hydrogels.

To gain insight into the antibacterial mechanism of the DNT hydrogel, SEM was utilized to study the morphological changes of bacteria. Both *E. coli* and *S. aureus* cells kept their original shape and intact structure, respectively (Figure 4a and Figure 4c). After treated with hydrogels, lysed bacteria and fused cells were clearly found owing to the total destruction of the membrane, respectively (Figure 4b and Figure 4d). In detail, the positively charged THPS released from DNT hydrogel is apt to adsorb onto the negative charged bacterial lipid membrane electrostatically, leading to a gradual lysis of membrane and the cell death eventually.[46] The contact-killing mechanism of THPS-induced membrane injury caused increased membrane permeability, supporting by the live/dead bacterial staining assay. *E. coli* and *S. aureus* bacteria were stained red after contacting with hydrogel (Figure 4f and Figure 4h) while little red color was found in cells without dealing with hydrogel (Figure 4e and Figure 4g), further proved that the DNT hydrogel destroyed the whole cell membrane. To sum up, THPS released from hydrogel largely affects the integrity and permeability of bacterial cell membrane, accounting for the antibacterial mechanism of the DNT hydrogel.

## Adhesion and rheological properties of DNT hydrogels.

Adhesion is an essential factor for tissue adhesive when hydrogels work as wound dressings. It has reported that −C=O, $-NH_2$ and −N= groups from nucleobases are able to form hydrogen bond by reacting with N, O, F, −OH, $-NH_2$ functional molecules or groups on the tissue surface.[47, 48] Therefore, we explored the adhesion property of DNT hydrogel and the result was illustrated in Figure 5a–5f, the hydrogel was able to adhere to the human skin, bottle cape, pipette tip and blazer, indicating the hydrogel possess certain adhesion. The features of the DNT hydrogel were closely dependent on its rheological properties, and then we inspected the viscosity modulus of the hydrogel. The viscosity value decreased from 1000 Pa to 5 Pa while the shear rate increased from 0.01 rad $s^{-1}$ to 10 rad $s^{-1}$, suggesting the hydrogel is imparted with shear-thinning, injectability properties (Figure 5g and Figure

5h). The ability to recover from external damages to keep original structural and functional integrity is vital for hydrogels when it comes to biomedical applications. We further assessed the strain-induced damage and self-healing property of the DNT hydrogel. The rheological strain sweep was conducted to test the responsive behavior of DNT hydrogel to external strains. With increasing strain from 0.01% to 1000% with a fixed frequency of 1 Hz at 25 °C and the Gel-to-Sol transition point occurred at 365%, suggesting the hydrogel collapsed (Figure 5i). The dynamic modulus of the hydrogel displayed a gel behavior under low strain at 0.1% and a sol state appeared when the strain hit 400%, 500%, 600%, 700% and 800%, and the rapid switches with over 90% recovery were found between sol and gel after 5 cycles of breaking and reforming (Figure 5j). This behavior was reversible and reproducible across the range of strains tested, illustrating DNT hydrogels possessed excellent self-healing performance due to the reversible nature of electrostatic interaction and hydrogen bonding. Besides, visual evidence of self-healing was displayed in Figure 5k–5n. These rheological and visual results together demonstrated that the adhesive DNT hydrogels with shear-thinning, injectability and self-healing have potential applications on soft materials injection, drug delivery and release.

### In vivo wound healing.

To demonstrate the potential application of DNT hydrogel to accelerate wound healing in vivo, we applied it in a mouse skin model owing to its certain adhesion, moist environment, antibacterial properties and biocompatibility. Such hydrogel was efficacious for bacteria elimination and wound healing, as visualized through the decreased wound size in Figure 6a. Unambiguously, wound treated with hydrogel was completely closed at the 15th day treatment while wounds treated by DNA+THPS (D+T) mixture and nontreated (BLANK) were not closed completely. These visual results illustrated that DNT hydrogel could be a wound dressing to suppress bacteria proliferation and accelerate the wound healing. Meanwhile, the images of the wound area were separated (Figure 6b) and their corresponding wound area ratios were calculated by Image Pro Plus shown in Figure 6c. The quantification results of wound area ratios of DNT hydrogel was approximate 0%, In contrast, about 7% and 20% for the (D+T) mixture and blank groups, respectively. All the results show that the wound treated with hydrogel recovered quicker than the other two counterparts treated with (D+T) mixture and nontreated. Taken together, the DNT hydrogel was capable of accelerating wound healing by providing a moist environment and releasing THPS to suppress the bacterial proliferation.

## CONCLUSION

In summary, we have prepared an adhesive and self-healing DNT hydrogel as a broad-spectrum wound dressing to against bacteria and accelerate wound healing. The hydrogel formation simultaneously took advantages of intermolecular electrostatic interaction and hydrogen bonding between DNA and THPS. The broad-spectrum antimicrobial mechanism was based on the disruption of bacterial cell membrane without detectable toxicity to mammalian cells. These results may indicate great potential of the DNT hydrogel as an antimicrobial material to accelerate wound healing and against wound infections. In the

meantime, the low cost and simple preparation may also make it attractive in biomedical field.

## EXPERIMENTAL SECTION

### Materials:

DNA from salmon tests, Propidium Iodide (PI) and Glutaraldehyde were purchased from Sigma Aldrich. THPS (ca: 70–80% in Water, MW 406.28) was purchased from Tokyo Chemical Industry Co., Ltd. SYTO™ 9 green fluorescent nucleic acid stain was purchased from ThermoFisher. Cell Counting Kit-8 (CCK-8) and Luria-Bertani (L-B) broth medium was purchased from Beyotime Biotechnology (Shanghai, China). Deionized water was used throughout the whole experiment. Roswell Park Memorial Institute 1640 (RPMI-1640) culture medium was purchased from Gibco ThermoFisher. *S. aureus and E. coli* strains were purchased from Shanghai Luwei Microbial Sci & Tech Co., Ltd.

### Characterizations:

Circular Dichroism (CD) Spectroscopy was performed on J-815 CD spectra (JASCO, Japan). UV-Vis was performed on a UV-Vis spectrophotometer (UV 2450, Shimadzu, Japan). Fourier transform infrared spectra (FT-IR) spectra was performed on Perkin Elmer Spectrum One Instrument (America). Rheological measurements were conducted on a rheometer (AR 2000ex, TA instrument, USA). Scanning electron microscopy (SEM) images were recorded using a NOVA nano SEM230 (FEI, USA), Live/dead bacterial staining assay was imaged using the Olympus BX-51 optical system microscope (Tokyo, Japan). The value of Optical Density (OD) was obtained by a microplate reader (ThermoFisher, USA). Liquid Chromatography-Mass Spectrometry (LC-MS) was performed on a mass spectrometer (Bruker Daltonics, Germany).

### Preparation of DNT hydrogel:

Typically, 4 wt% DNA was dissolved in deionized water and heated at 90 °C for about 20 min, then 50 μL 50 mg $mL^{-1}$ THPS was added to DNA solution and stirred vigorously, a transparent DNT hydrogel was obtained.

### SEM study of hydrogels:

Scanning electron microscopy (SEM) was utilized to study the morphology of the obtained hydrogels. Hydrogel samples were freeze-dried by a freezer and then placed on a silicon wafer. Finally, sputter coated with gold before imaged by SEM.

### Rheological studies of DNT hydrogel:

Rheological measurements were performed on a rheometer. Hydrogel samples were placed on the rheometer stage, a dynamic frequency sweeping from 0.1 to 10 Hz under the strain at 1% at 25 °C. Viscosity of the hydrogel with increasing shear rate from 0.01 to 10 rad $s^{-1}$ by continuous flow experiment was conducted under the strain at 1% at 25 °C. Dynamic modulus of hydrogel under increasing strain with a fixed frequency of 1 Hz at 25 °C.

### Spectrum characterizations of hydrogels:

CD spectra was scanned between 200 and 350 nm with an interval of 0.2 nm. UV-vis were scanned between 200 and 350 nm with an interval of 0.5 nm. FT-IR spectra was scanned between 500 and 1800 $cm^{-1}$ with an interval of 1 $cm^{-1}$.

### Bacteria culture:

Bacteria of *S. aureus* (CMCC 26003) and *E. coli* (ATCC 25922) strains were used in our experiment. Before the experiment, the bacteria were grown overnight at 37 °C at 180 rmp $s^{-1}$ and harvested at the exponential growth phase via centrifugation at 4000 rmp $s^{-1}$ for 5 min and washed with PBS for 3 times. The supernatant was then discarded and the cell pellet was resuspended in PBS. For LB solid medium plates culture, 10 μL bacteria solution was added on solid medium and the pure LB solid medium was used as a control, and then placed on an incubator at 37 °C for 24 h. For time-dependent antibacterial experiment, the bacteria concentration was monitored photometrically by measuring the $OD_{600}$ value. Prior to conducting the antibacterial experiment with the hydrogels, the $OD_{600}$ value of the bacteria solution was obtained. Then, 1 mL *S. aureus* and *E. coli* bacteria solution were contacted with the DNT hydrogel, DNA (2 wt%) solution and THPS (1 $mg.mL^{-1}$) solution respectively. For concentration-dependent antibacterial experiment, 1 mL *S. aureus* and 1 mL *E. coli* bacteria solution with different bacteria concentrations ($1\times10^4$ to $1\times10^9$ CFU $mL^{-1}$) were contacted with the surface of the hydrogels for 24 h, respectively. Their $OD_{600}$ values were obtained by a microplate reader and the bacteria solution without hydrogel was used as control.

### Cytotoxicity assay:

The cytotoxicity of hydrogel against L929 cells was investigated by CCK-8 assay. Cells were cultured in RPMI-1640 culture medium with 10% fetal bovine serum and 1% penicillin-streptomycin at 37 °C in a humidified atmosphere of 5% $CO_2$. $2\times10^5$ cells were cultured in 96-wells plate for 24 h, then DNT hydrogel was added and further cultured for another 24 h and 48 h. Finally, 10 μL CCK-8 solution was added and incubated for 2 h before measuring the value of $OD_{450}$.

### SEM image of bacteria:

Bacteria treated with hydrogel before or after were harvested at 4000 rmp $s^{-1}$ for 5 min and washed with PBS for 3times, and then fixed in PBS containing 2.5% glutaraldehyde for 2 h at room temperature. The bacteria were further washed with PBS and dehydrated by a series of ethanol solutions (20%, 40%, 60%, 80% and 100%) for 10 min with each step. Finally, the bacteria were placed on the silicon wafer and dried via freeze-dried at the room temperature, and then sputter coated with gold and imaged with SEM.

### Live/Dead staining analysis:

Bacteria incubated with or without hydrogel for 12 h, and then the bacteria solution was treated with 1 μL of 1 μM SYTO™ 9 and 10 μL of 1 mg $mL^{-1}$ PI for 1 h. Next, the bacteria solution was further washed with PBS for 3 times, and followed by imaging by fluorescence microscope.

### Mouse injury model:

To estimate the effect of the hydrogel for wound healing, injury model was built on back of mouse. The Balb/c mice (6–8 weeks) back were shaved and 1 centimeter long cross wound was made on the back of the tested mice. The mice were divided into 3 groups (three per groups). Before constructing the wound model, mice were weighed and anesthetized using Pentobarbital sodium (60 μL, 20 kg $mL^{-1}$). The wound was treated with D+T mixture (60 μL) and nontreated as two control groups and DNT hydrogel (60 μL) as the experimental group. Subsequently, they were individually housed in cages and equivalent food and water were supplied to them under constant temperature. Wound healing progression was digitally recorded every four days. The mice were successively observed and fed for 15 days to study the wound healing progression. All the test mice were with approval of the Xiangya School of Medicine, Central South University. The animal experiment and animal care were conducted in the Xiangya School of Medicine and the authors followed the rules and ethical protocols strictly in the whole animal procedures.

## Supplementary Material

Refer to Web version on PubMed Central for supplementary material.

## ACKNOWLEDGEMENT

The authors thank the support of this work by the National Natural Science Foundation of China (Grant No.21575165)

## REFERENCES

(1). Oliver JD, Wound infections caused by Vibrio vulnificus and other marine bacteria. Epidemio. Infect 2005, 133, 383–391.

(2). Suzuki M; Yamada K; Nagao M; Aoki E; Matsumoto M; Hirayama T; Yamamoto H; Hiramatsu R; Ichiyama S; Iinuma Y, Antimicrobial ointments and methicillin-resistant Staphylococcus aureus USA300. Emerg. Infect. Dis 2011, 17, 1917–20. [PubMed: 22000371]

(3). Agnihotri S; Mukherji S; Mukherji S, Immobilized silver nanoparticles enhance contact killing and show highest efficacy: elucidation of the mechanism of bactericidal action of silver. Nanoscale 2013, 5, 7328–7340. [PubMed: 23821237]

(4). Ramyadevi J; Jeyasubramanian K; Marikani A; Rajakumar G; Rahuman AA, Synthesis and antimicrobial activity of copper nanoparticles. Mater. Lett 2012, 71, 114–116.

(5). Zheng KY; Setyawati MI; Leong DT; Xie JP, Antimicrobial Gold Nanoclusters. ACS Nano 2017, 11, 6904–6910. [PubMed: 28595000]

(6). Veerasubramanian PK; Thangavel P; Kannan R; Chakraborty S; Ramachandran B; Suguna L; Muthuvijayan V, An investigation of konjac glucomannan-keratin hydrogel scaffold loaded with Avena sativa extracts for diabetic wound healing. Colloid. Surface B 2018, 171, 319–319.

(7). Yacoby I; Bar H; Benhar I, Targeted drug-carrying bacteriophages as antibacterial nanomedicines. Antimicrob. Agents Ch 2007, 51, 2156–2163.

(8). Qiu XQ; Zhang H; Wang H; Wu GY, A novel engineered peptide, a narrow-spectrum antibiotic, is effective against vancomycin-resistant Enterococcus faecalis. Antimicrob. Agents Ch 2005, 49, 1184–1189.

(9). Drury JL; Mooney DJ, Hydrogels for tissue engineering: scaffold design variables and applications. Biomaterials 2003, 24, 4337–4351. [PubMed: 12922147]

(10). Tibbitt MW; Anseth KS, Hydrogels as Extracellular Matrix Mimics for 3D Cell Culture. Biotechnol. Bioeng 2009, 103, 655–663. [PubMed: 19472329]

(11). Hoare TR; Kohane DS, Hydrogels in drug delivery: Progress and challenges. Polymer 2008, 49, 1993–2007.

(12). Kopecek J, Hydrogels: From Soft Contact Lenses and Implants to Self-Assembled Nanomaterials. J. Polym. Sci. Pol. Chem 2009, 47, 5929–5946.

(13). Zhai MC; Xu YC; Zhou B; Jing WB, Keratin-chitosan/n-ZnO nanocomposite hydrogel for antimicrobial treatment of burn wound healing: Characterization and biomedical application. J. Photoch. Photobio. B 2018, 180, 253–258.

(14). Wu F; Meng GL; He J; Wu Y; Wu F; Gu ZW, Antibiotic-Loaded Chitosan Hydrogel with Superior Dual Functions: Antibacterial Efficacy and Osteoblastic Cell Responses. ACS Appl. Mater. Inter 2014, 6, 10005–10013.

(15). Mahata D; Nag A; Nando GB; Mandal SM; Franco OL, Self-Assembled Tea Tannin Graft Copolymer as Nanocarriers for Antimicrobial Drug Delivery and Wound Healing Activity. J. Nanosci. Nanotechno 2018, 18, 2361–2369.

(16). Loh EYX; Mohamad N; Fauzi MB; Ng MH; Ng SF; Amin MCIM, Development of a bacterial cellulose-based hydrogel cell carrier containing keratinocytes and fibroblasts for full-thickness wound healing. Sci. Rep 2018, 8(1).2875. [PubMed: 29440678]

(17). El-Kased RF; Amer RI; Attia D; Elmazar MM, Honey-based hydrogel: In vitro and comparative In vivo evaluation for burn wound healing. Sci. Rep 2017, 7(1),9692. [PubMed: 28851905]

(18). Park N; Um SH; Funabashi H; Xu JF; Luo D, A cell-free protein-producing gel. Nature Materials 2009, 8, 432–437. [PubMed: 19329993]

(19). Shin M; Ryu JH; Park JP; Kim K; Yang JW; Lee H, DNA/Tannic Acid Hybrid Gel Exhibiting Biodegradability, Extensibility, Tissue Adhesiveness, and Hemostatic Ability. Adv. Funct. Mater 2015, 25, 1270–1278.

(20). Nishikawa M; Ogawa K; Umeki Y; Mohri K; Kawasaki Y; Watanabe H; Takahashi N; Kusuki E; Takahashi R; Takahashi Y; Takakura Y, Injectable, self-gelling, biodegradable, and immunomodulatory DNA hydrogel for antigen delivery. J. Control Release 2014, 180, 25–32. [PubMed: 24530618]

(21). Zhang L; Lei JP; Liu L; Li CF; Ju HX, Self-Assembled DNA Hydrogel as Switchable Material for Aptamer-Based Fluorescent Detection of Protein. Anal. Chem 2013, 85, 11077–11082. [PubMed: 24138007]

(22). Song J; Im K; Hwang S; Hur J; Nam J; Ahn GO; Hwang S; Kim S; Park N, DNA hydrogel delivery vehicle for light-triggered and synergistic cancer therapy. Nanoscale 2015, 7, 9433–9437. [PubMed: 25959856]

(23). Ma XZ; Yang ZQ; Wang YJ; Zhang GL; Shao Y; Jia HY; Cao TY; Wang R; Liu DS, Remote Controlling DNA Hydrogel by Magnetic Field. ACS Appl. Mater. Inter 2017, 9, 1995–2000.

(24). Li C; Faulkner-Jones A; Dun AR; Jin J; Chen P; Xing YZ; Yang ZQ; Li ZB; Shu WM; Liu DS; Duncan RR, Rapid Formation of a Supramolecular Polypeptide-DNA Hydrogel for In Situ Three-Dimensional Multilayer Bioprinting. Angew. Chem. Int. Ed 2015, 54, 3957–3961.

(25). Tang H; Duan X; Feng X; Liu L; Wang S; Li Y; Zhu D, Fluorescent DNA-poly(phenylenevinylene) hybrid hydrogels for monitoring drug release. Chem. Commun 2009, 641–643.

(26). Costa D; Queiroz J; Miguel MG; Lindman B, Swelling behavior of a new biocompatible plasmid DNA hydrogel. Colloid. Surface B 2012, 92, 106–112.

(27). Truong NP; Jia Z; Burgess M; Payne L; Mcmillan NAJ; Monteiro MJ, Self-Catalyzed Degradable Cationic Polymer for Release of DNA. Biomacromolecules 2011, 12, 3540. [PubMed: 21838265]

(28). Strekowski L; Wilson B, Noncovalent interactions with DNA: an overview. Mutat. Res 2007, 623, 3–13. [PubMed: 17445837]

(29). Topuz F; Singh S; Albrecht K; Möller M; Groll J, DNA Nanogels To Snare Carcinogens: A Bioinspired Generic Approach with High Efficiency. Angew. Chem. Int. Ed 2016, 55, 12210–12213.

(30). Jia R; Li Y; Al-Mahamedh HH; Gu T, Enhanced Biocide Treatments with D-amino Acid Mixtures against a Biofilm Consortium from a Water Cooling Tower. Front Microbiol 2017, 8, 1538. [PubMed: 28861053]

(31). Li P; Li H; Li J; Guo X; Liu J; Xiao B, Evaluation of sludge reduction of three metabolic uncouplers in laboratory-scale anaerobic-anoxic-oxic process. Bioresour. Technol 2016, 221, 31–36. [PubMed: 27639221]

(32). Guo X; Yang J; Liang Y; Liu J; Xiao B, Evaluation of sludge reduction by an environmentally friendly chemical uncoupler in a pilot-scale anaerobic/anoxic/oxic process. Bioproc. Biosyst. Eng 2014, 37, 553–60.

(33). Xu D; Wen J; Fu W; Gu T; Raad I, D-amino acids for the enhancement of a binary biocide cocktail consisting of THPS and EDDS against an SRB biofilm. World J. Microbiol. Biotechnol 2012, 28, 1641–6. [PubMed: 22805946]

(34). Xu D; Li Y; Gu T, A synergistic D-tyrosine and tetrakis hydroxymethyl phosphonium sulfate biocide combination for the mitigation of an SRB biofilm. World J. Microbiol. Biotechnol 2012, 28, 3067–74. [PubMed: 22806745]

(35). Connor TH; Meyne J; Legator MS, The mutagenic evaluation of tetrakis (hydroxymethyl) phosphonium sulfate using a combined testing protocol approach. J. Environ. Pathol. Tox 1980, 4, 145–158.

(36). Downward B; Talbot R; Haack T, TetrakisHydroxymethylPhosphonium Sulfate (THPS) A New Industrial Biocide With Low Environmental Toxicity. Corrosion 1997.

(37). Moore DS, Double-helical DNA and RNA circular dichroism. Biopolymers 1974, 13.

(38). Privé GG; Heinemann U; Chandrasegaran S; Kan LS; Kopka ML; Dickerson RE, Helix geometry, hydration, and G.A mismatch in a B-DNA decamer. Science 1987, 238, 498. [PubMed: 3310237]

(39). Tanaka K; Okahata Y, A DNA-lipid complex in organic media and formation of an aligned cast film. J. Am. Chem. Soc 1996, 118, 10679–10683.

(40). Wolf B; Hanlon S, Structural transitions of deoxyribonucleic acid in aqueous electrolyte solutions. II. The role of hydration. Biochemistry 1975, 14, 1661–1670. [PubMed: 1168490]

(41). Zhou C-Y; Xi X-L; Yang P, Studies on DNA binding to metal complexes of Sal2trien. Biochemistry 2007, 72, 37–43. [PubMed: 17309435]

(42). Nafisi S; Adelzadeh M; Norouzi Z; Sarbolouki MN, Curcumin binding to DNA and RNA. DNA. Cell Bio 2009, 28, 201–208. [PubMed: 19364279]

(43). Ouameur AA; Tajmir-Riahi HA, Structural Analysis of DNA Interactions with Biogenic Polyamines and Cobalt(III)hexamine Studied by Fourier Transform Infrared and Capillary Electrophoresis. J. Biol. Chem 2004, 279, 42041–42054. [PubMed: 15284235]

(44). Choosakoonkriang S; Wiethoff CM; Koe GS; Koe JG; Anchordoquy TJ; Middaugh CR, An Infrared Spectroscopic Study of the Effect of Hydration on Cationic Lipid/DNA Complexes. J. Pharm. Sci 2003, 92, 115–130. [PubMed: 12486688]

(45). Gunasekaran S; Kumaresan S; Balaji RA; Anand G; Seshadri S, Vibrational spectra and normal coordinate analysis on structure of chlorambucil and thioguanine. Pramana 2008, 71, 1291–1300.

(46). Yang Y; Cai Z; Huang Z; Tang X; Zhang X, Antimicrobial cationic polymers: from structural design to functional control. Polym. J 2017, 50, 33–44.

(47). Cheng S; Zhang M; Dixit N; Moore RB; Long TE, Nucleobase Self-Assembly in Supramolecular Adhesives. Macromolecules 2012, 45, 805–812.

(48). Heinzmann C; Weder C; de Espinosa LM, Supramolecular polymer adhesives: advanced materials inspired by nature. Chem. Soc. Rev 2016, 45, 342–358. [PubMed: 26203784]

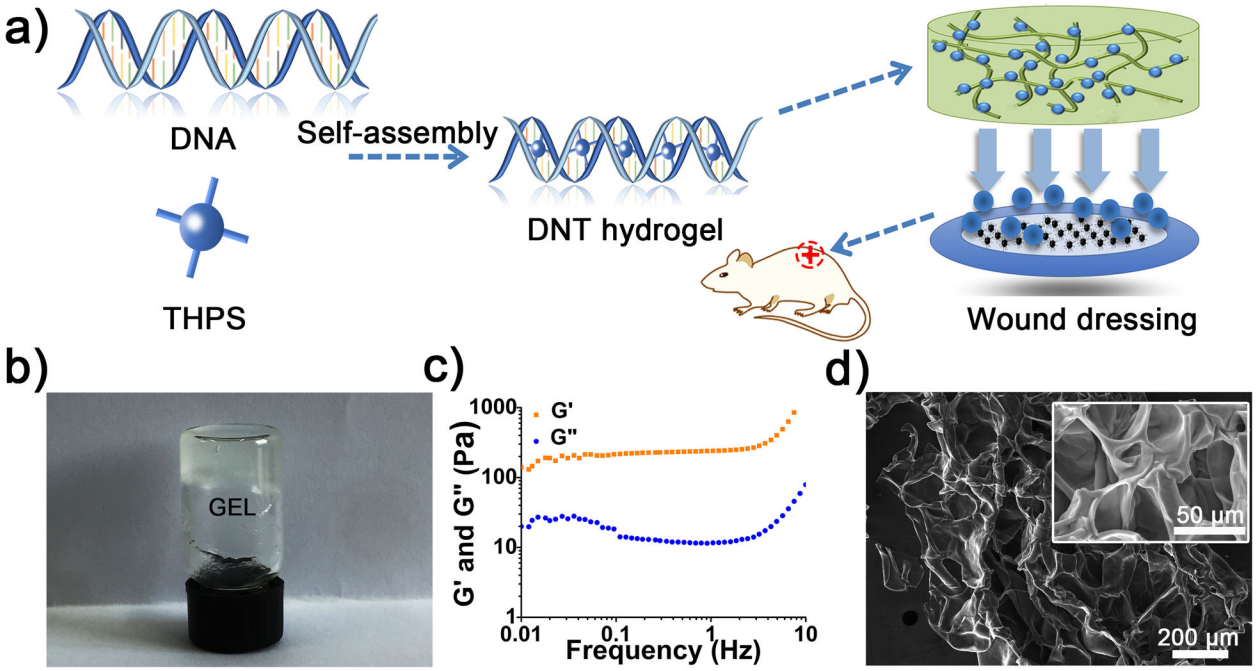


**Figure 1.**

a) Schematic representation of formation of the self-assembled DNT hydrogel. b) The photograph of DNT hydrogel. c) Frequency-dependent oscillatory rheology of the DNT hydrogel. d) SEM images of the hydrogel indicated the formation of intertwined network and porous structure.

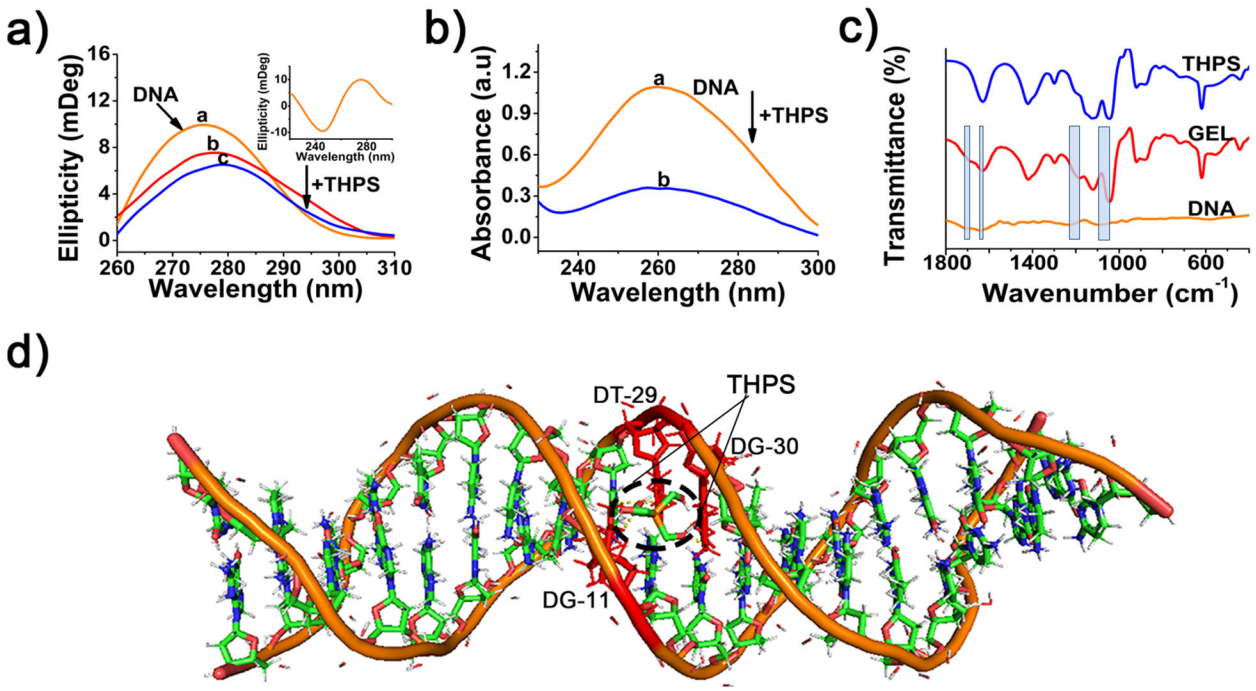


**Figure 2.**

a) CD spectra of DNA and DNA-THPS complex, different concentration of THPS mixed with DNA, from curves a to care corresponding to 0, 10, 50 mg $mL^{-1}$ and concentration of DNA is 0.5 wt%. b) UV-vis absorption spectra of DNA and DNA-THPS complex, a and b are DNA and DNA-THPS, respectively. DNA concentration is 0.05 wt% and THPS concentration is 10 mg $mL^{-1}$. c) FTIR spectra of the freeze-dried DNA solution, DNT hydrogel and THPS solution, the width of rectangles stands for the shift of wavenumbers. d) Molecular Docking simulation of the binding site between DNA and THPS.

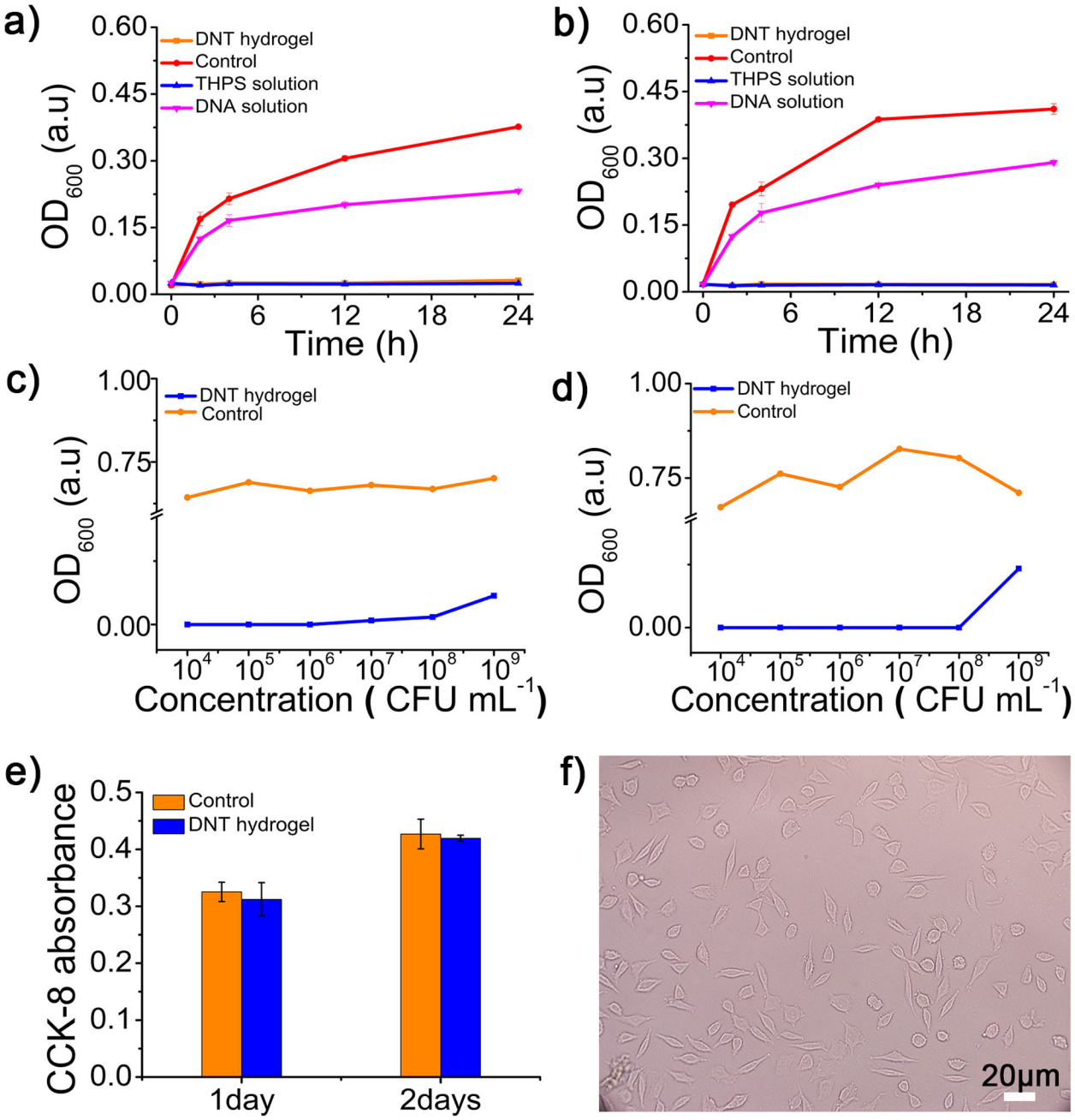


**Figure 3.**

Time-dependent antibacterial effects of the DNT hydrogel against $1\times10^7$ CFU $mL^{-1}$ a) *S. aureus* and b) *E. coli*. Concentration-dependent antibacterial effect of the hydrogel toward c) *S. aureus* and d) *E. coli*, different concentration of *S. aureus* and *E. coli* bacteria were incubated with the hydrogel for 24 h. e) The CCK-8 activity of L929 cells contacted with DNA hydrogel from 1 to 2 days. f) The shape of L929 cells treated with DNT hydrogel showed on fluorescence microscope

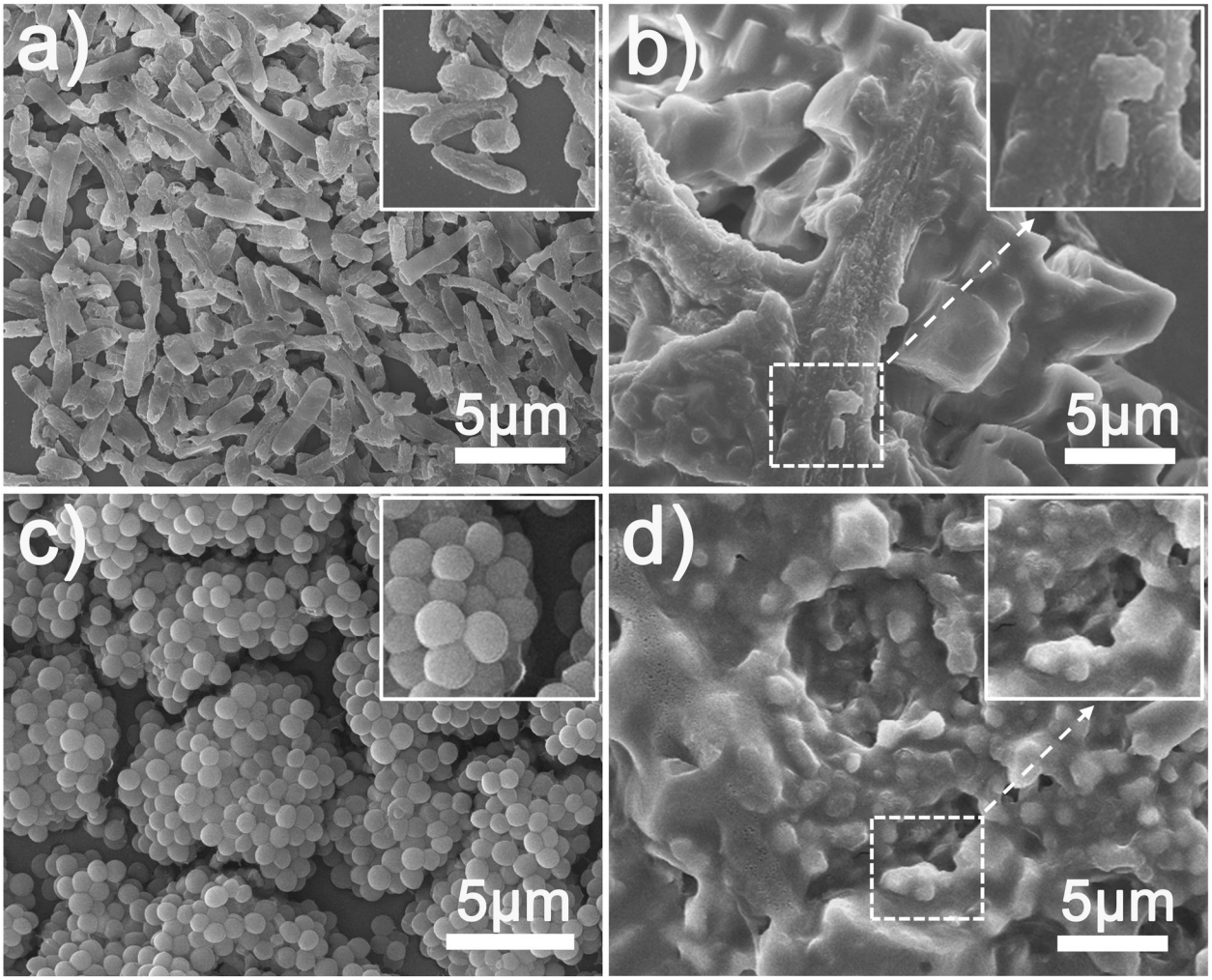


**Figure 4.**

I) Representative SEM images of E. coli before a) and after b) contact with the hydrogel for 12 h, SEM images of S. aureus before c) and after d) contact with the hydrogel for 12 h. II) Overlapping fluorescence images for live/dead bacterial staining assay of E. coli before e) and after f) contact with the hydrogel, overlapping fluorescence images for live/dead assay of S. aureus before g) and after h) contact with the hydrogel.

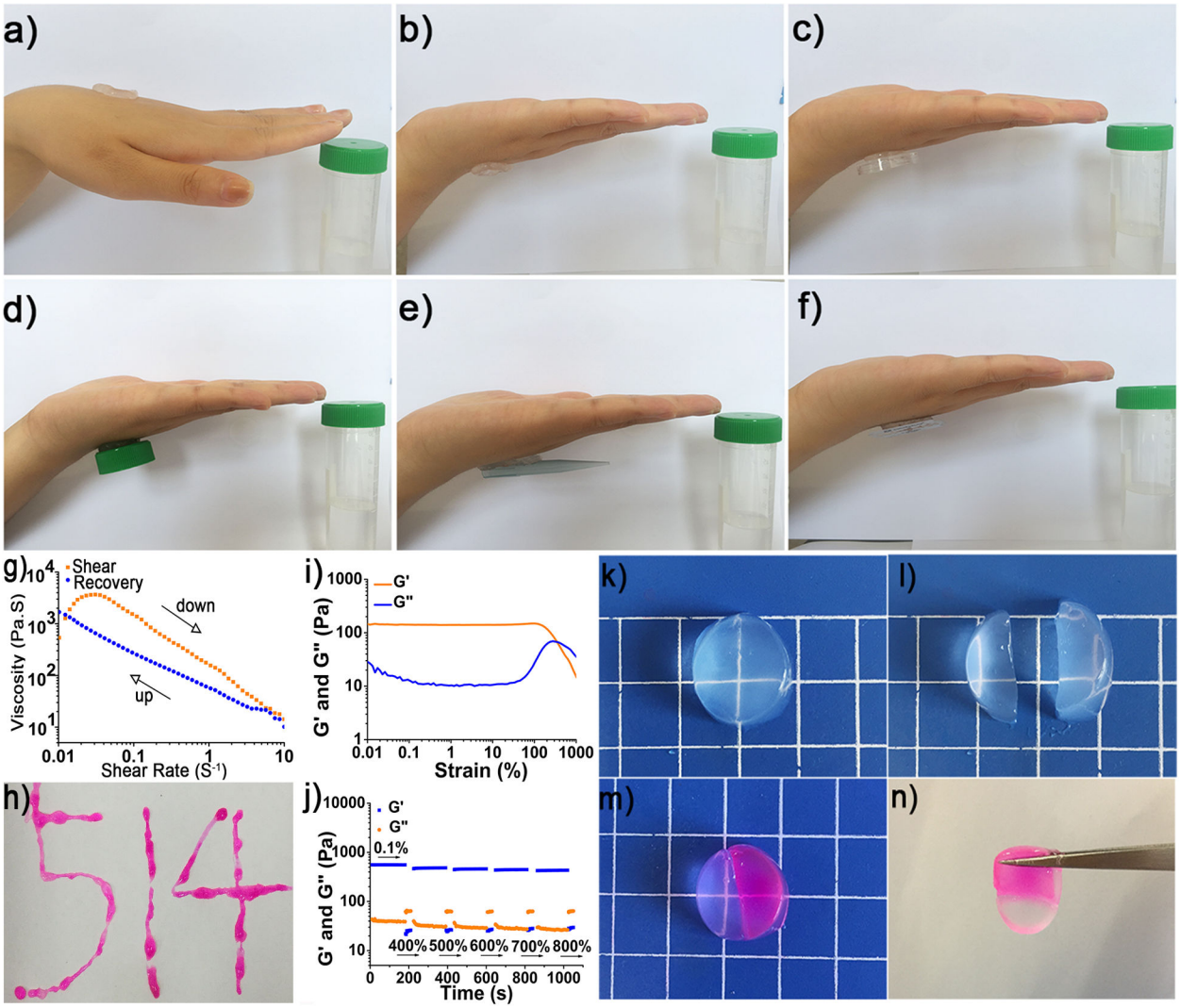


**Figure 5.**

Adhesive exhibition of DNT hydrogel, adhering to human skin a) and b), a bottle cap c) and d), pipette tip e) and blazer f). g) Viscosity as a function of shear rate. h) The injectable property of the hydrogel. i) Dynamic modulus of DNT hydrogel under increasing strains from 0.01% to 1000% with a fixed frequency of 1 Hz at 25 °C. j) The dynamic modulus of hydrogel under low strain (0.1%) and high strain (400%, 500%, 600%, 700% and 800%). A hydrogel sample k) was cut in half l), and one was stained with rhodamine and then two fragments were brought together after several minutes m), then heal into one n).

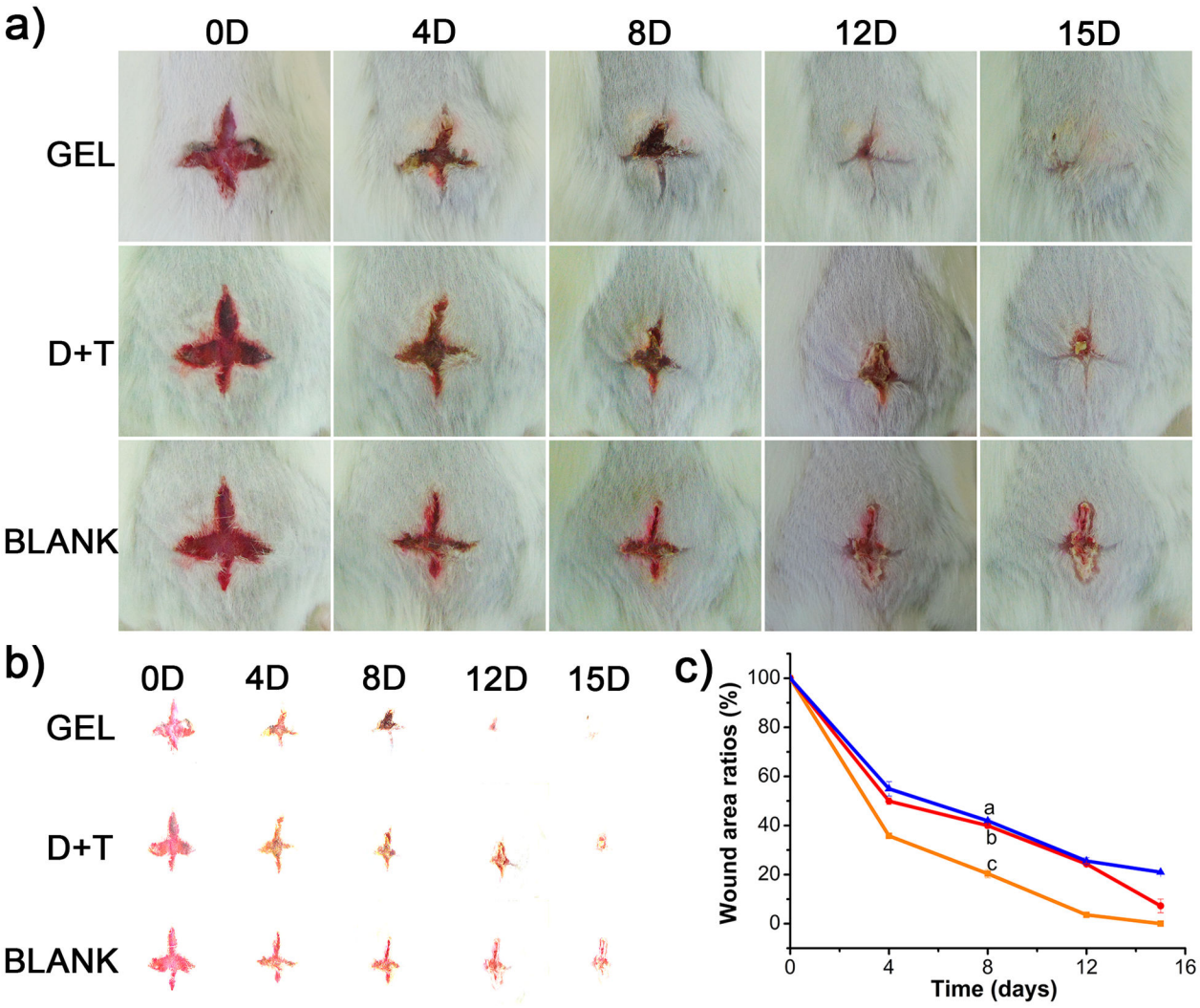


**Figure 6.**

a) Photographs of the wounds treated with hydrogels, (D+T) mixture and nontreated at 0, 4, 8, 12 and 15 days respectively. b) Separation image of the wound area. c) The wound area was measured by Image Pro Plus and the plot of wound area ratio, from curve a to c, BLANK, (D+T) mixture, DNT hydrogel.